

FACTA UNIVERSITATIS

Series: **Electronics and Energetics** Vol. 28, N° 1, March 2015, pp. 29 - 50

DOI: 10.2298/FUEE1501029N

EXAMPLES OF MEDICAL SOFTWARE AND HARDWARE EXPERT SYSTEMS FOR DYSFUNCTION ANALYSIS AND TREATMENT

**Andrzej Napieralski, Zygmunt Ciota, Marcin Janicki,
Marek Kamiński, Rafał Kotas, Paweł Marciniak,
Aleksander Mielczarek, Małgorzata Napieralska, Robert Ritter,
Bartosz Sakowicz, Wojciech Tylman, Mariusz Zubert**

Lodz University of Technology, Department of Microelectronics and Computer Science,
Lodz, Poland

Abstract. *This paper presents the recent research in DMCS. The medical and biometric research projects are presented. One of the key elements is image acquisition and processing. The paper presents research of diagnostic application of voice analysis for stroke patients with speech dysfunction, as well as the method for diagnosing and monitoring the effectiveness of medical rehabilitation of patients with dysfunction of the cervical spine. Then the method for sudden cardiac death risk stratification is elaborated.*

Key words: *medical systems, speech dysfunction, sudden cardiac death risk*

1. RESEARCH OF DIAGNOSTIC APPLICATION OF VOICE ANALYSIS FOR STROKE PATIENTS WITH SPEECH DYSFUNCTION

Human verbal communication presents a very complex process, consisting of nervous impulse synchronization, stimulation of speech processes, extraction of phonetic information by using an aural system. The tracking process of speech context, occurring in the brain, also presents a very important task of neural network activation. Subjective diagnosis carried out by an experienced phoniatriest or speech therapist is the simplest method of a voice quality evaluation. Such classification of voice requires experience and intuition, it cannot be applied commonly, especially in comparative studies presented by various medical centres.

A better technique of measurements of voice quality can be obtained applying an objective acoustic analysis, a relatively new method. Spectrographic, sonographic and temporary analyses of speech signals are useful as objective methods of voice quality measurements. Computer modelling of such complicated process demands a large number of mathematical calculations performed by high-speed processors. In the case of vascular

Received October 30, 2014

Corresponding author: Andrzej Napieralski

Lodz University of Technology, Department of Microelectronics and Computer Science, ul. Wolczanska 221/223,
90-924 Lodz, Poland

(e-mail: napier@dmcs.pl)

lesion of nervous areas, additional pathological distortions should be taken into account as dominant parameters. Evaluation of importance of such parameters demands close collaboration between neurologists, computer scientists and electronic engineers. Such collaboration gives us opportunity to verify a possibility of treatment progress of the patient using our new signal-statistical method.

The correlation between pathological changes of neurological stability and voice pathology can be established. To obtain rewarding results, different analyses must be implemented: time domain, frequency domain and mixed time-frequency analysis, all of which should be assisted by statistical functions for the calculation of voice variability as a function of health state.

One of the most important tasks is a proper definition of feature vectors. Each vector can contain several specific features of voice signals, and finally, one has to calculate more than hundred features for each utterance. The following four vectors can be favoured as very important and useful, covering the most important features of speech signal: long-term spectra (LTS) vector, speaking fundamental frequency vector, time-energy distribution vector and vowel formant-tracking vector [1]. To obtain such vectors, two kind of analysis should be taken into account:

- Long Term Analysis Spectrum –voice samples are relatively long (a few seconds),
- Short Term Analysis, applying Fast Fourier Transformation – it contains short intervals of the speech (from 0.1 to 0.6 seconds).

We present a new method of registration and processing of voice parameters for patients with vascular lesion of a central nervous system. The most frequent cause of it are strokes, where one can observe focal disorders of the cerebrum functions caused by vascular injury. There are two kinds of stroke: hemorrhagic (20% of all cases) and ischaemic (80% of all cases in medical practice). The speech quality depends on programming action of the central nervous arrangement and the condition of the broadcast of stimuli in cortical-subcortical area.

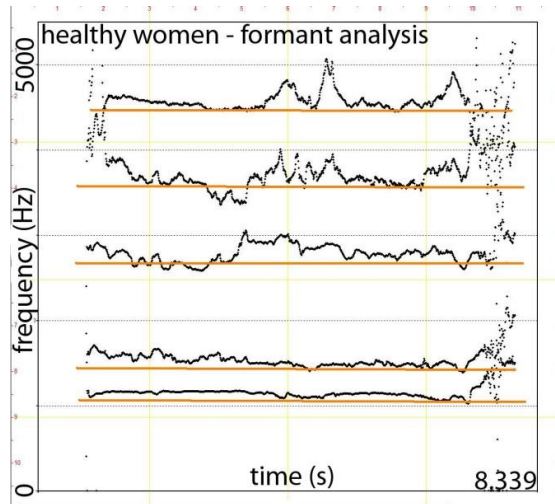
Voice analysis has been performed by using our own algorithms of signal processing based on Fourier transforms. Additionally, statistical analysis was used to obtain proper correlation between the improvement of voice parameters and neurological condition of the examined patient. The investigations were performed for several patients with ischemic and also hemorrhagic stroke, during the first three days of hospitalization. Afterwards, next examinations were repeated once a week.

The voice analysis of the patients with ischemic brain stroke, performed by using our software, indicated specific deviations of frequency and amplitude in the formant parameters (the phoneme ‘a’ seems to be very important example), in comparison with healthy persons. The same abnormalities were significantly smaller for patients with aphasia in the case of the hemorrhagic stroke. The presented method permits establishing a possibility of speech recovery process just at the beginning of the ischemic stroke.

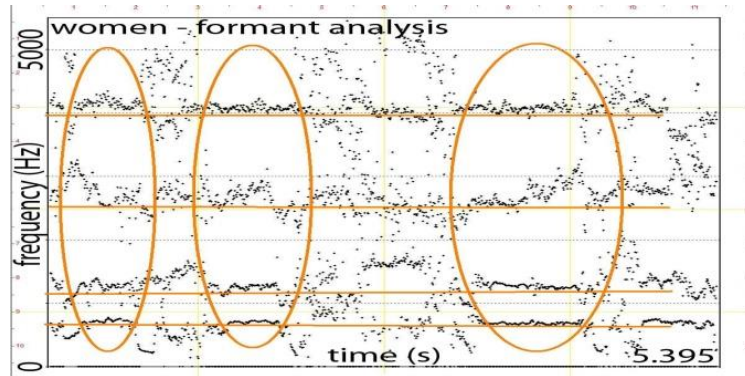
We record patients and next we analyse these samples by using various algorithms. Numerical data are assigned to the patient’s state of health during the recording and are compared with data of a healthy human of the same age group and gender. We use time, frequency and time-frequency analysis.

It is possible to observe the characteristic changes as a function of the patient health state. These dependences are proportional to the degree the cerebrum damages. The

characteristic of spectral estimation of a healthy person has the soft course. For ill persons the power of the signal is characterized by larger amplitudes. The examples of the results are presented in Fig. 1, 2 and 3 [2, 3].



Transient ischaemia - 2nd day in hospital



Transient ischaemia - 7th day in hospital

Fig. 1 Voice signal processing for the patient with stroke hospitalization - mixed time-frequency (formant) analysis

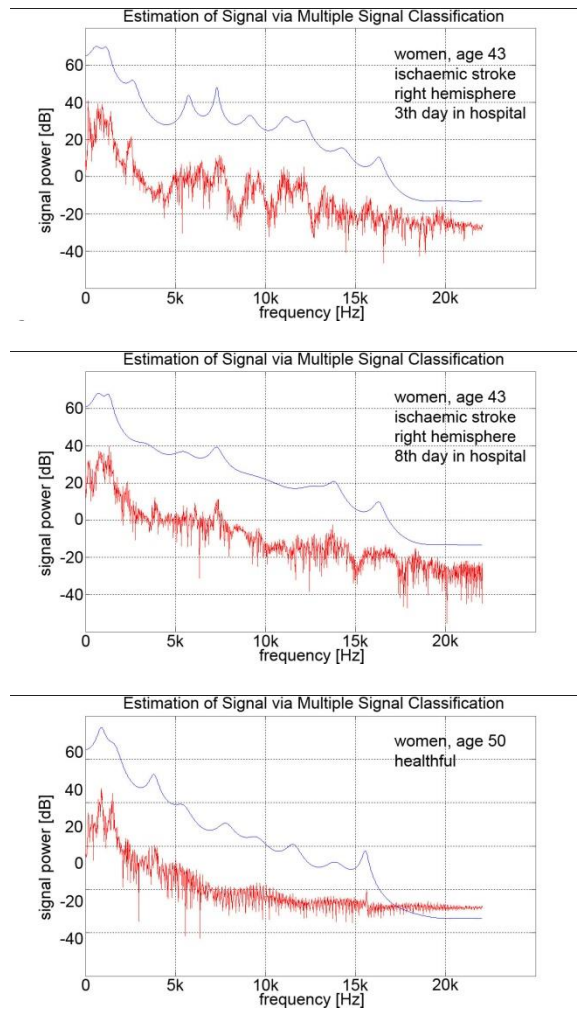


Fig. 2 Voice signal processing for patients with stroke hospitalization - frequency domain results [2]

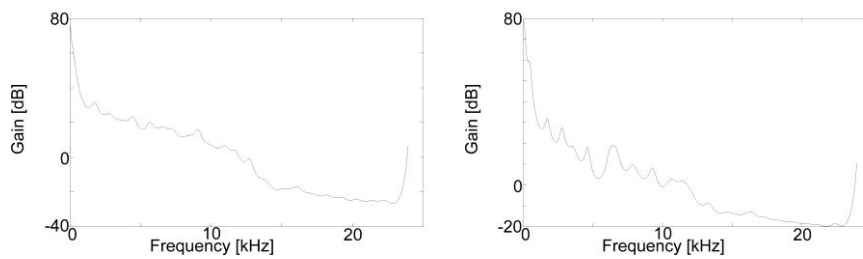


Fig. 3 Vocal track filter for the patient with traumatic haematoma in the left and right hemisphere in the first (left) and last (right) day of hospitalization [3]

2. AN INNOVATIVE METHOD FOR DIAGNOSING AND MONITORING THE EFFECTIVENESS OF MEDICAL REHABILITATION OF PATIENTS WITH DYSFUNCTION OF THE CERVICAL SPINE

2.1. The examination process

2.1.1 The former procedure

The traditional method of examination requires attaching a laser pointer to the patient's head, which is done by using fixture based on tightly fitting ear protectors. The examinee is sitting in front of a white screen with several colour shapes drawn on it – the setup is outlined in Fig. 4. The medical doctor is observing how fast and accurately the patient is following the shapes with the spot of the laser. This method requires the doctor to stay firmly focused for about ten minutes, during which he/she assesses the quality and time of completion of subsequent tasks.

Reduction of human engagement in the process of data acquisition should make the assessment more precise and repeatable. Estimation of the accuracy, with which the examinee is able to operate the spot, evaluation of the scope of the screen that the patient is able to reach and time measurement are tasks that are proved to be successfully performed by the computers. Moreover, the digital storage of the results will in the future facilitate tracking progress in rehabilitation and will help design new exercises tailored to the individual patient's needs.

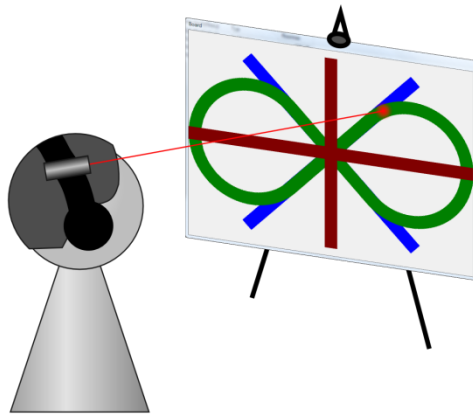


Fig. 4 Former examination procedure

skeletal muscles per second [4]. People training the same move on a daily basis may double or even triple this value, but such a situation may be neglected in case of the head. However, since the movements are generally nonlinear, several higher harmonics shall also be taken into account. Inclusion of the first three harmonics implicates the sampling rate reaching about 90 measurements per second (to fulfil Nyquist equation for three first harmonics of body part moving with 15 Hz fundamental frequency).

The device shall not indicate a drift of the pointer larger than 2 mm during a 10-minute time period of being at rest.

2.1.2 Requirements for automated test

The measurement method has to fulfil several types of constraints, these are: accuracy, bandwidth and reproducibility of results. All these fields were initially discussed with medical doctors.

The measurement setup is expected to achieve the resolution of about 1 mm with a patient sitting or standing about three meters away from the screen. The desired accuracy is hence similar to the one achieved by a person observing the screen during the original examination procedure.

A typical man is able to perform up to about 15 cycles of tensing and relaxing of

2.1.3 The proposed measuring method

The adopted approach is founded on the assumption that it is possible to calculate the laser pointer location on the screen based on the limited knowledge of the patient's head position. The task could be easily accomplished if the head position (three coordinates) and angles (at least two) in relation to the screen would be known with appropriate accuracy. The problem could be then brought to projection of a point on a plane along a predefined line.

In practice, the precise measurement of the actual head position is complicated and the applicable techniques are expensive. Therefore, the proposed system shall be able to operate without obtaining those parameters directly. The measurement of angles is more straightforward, as there are numerous sensors available that can directly or indirectly provide the elevation and heading angle.

A convenient way to measure the required angles is to fix a device with sensors to the

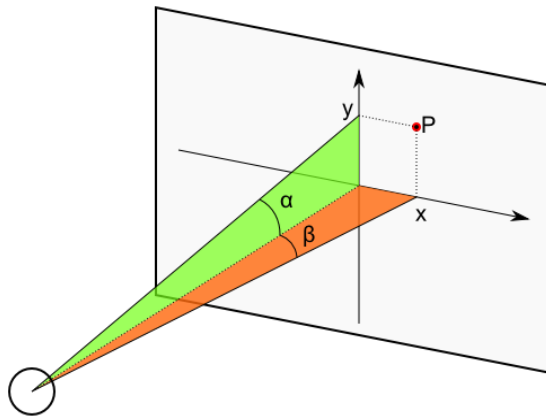


Fig. 5 Spot projection on the screen

patient's head, in the same manner as the laser pointer was originally mounted. Measurement of the elevation angle (labelled α in Fig. 5) is relatively simple as it requires only determining the direction of the Earth's gravitational force vector in the coordinate system of the device and thus the head. The market available inclinometers, sensors dedicated for this measurement, are relatively expensive. Alternatively, the α angle can be determined using an accelerometer accompanied with angle computation procedures implemented in the software.

The measurement of rotation in the horizontal plane (β) cannot be done analogically, as the g -force vector is constant during such a movement. Apart from gravity, the Earth is also a source of magnetic field, which might be used to determine the patient heading with the utilization of magnetometer. Unfortunately, this field is very weak and the local induction vector depends heavily on the nearest environment. It can vary significantly even in a short term observation, for example due to nearby electrical appliances. The system could never fully rely on the magnetometer readouts.

Another method of determining both angles is the measurement of angular velocities of the device using a gyroscope. Integrating these will directly lead to the angle values. This method is simple, but has several important drawbacks. Any sensor error will be integrated over time causing a constant drift of the angle value. Moreover, the integration constant is not known in advance. Nevertheless, the gyroscope is more reliable than the magnetometer and it is utilized in the proof-of-concept device. Both problems indicated above had to be solved to take the full benefit of this sensor's features.

The drift of calculated angles can be significantly reduced by calibrating the sensor before the examination. The system can determine the constant component continuously present on gyroscope outputs and cancel it out during the actual measurement.

The described projection implementation was intended to be temporary, which should be corrected just after the application becomes functional. Unexpectedly, this solution seems to be accurate enough for system evaluation purposes and initial tests on patients. There is a visible deviation between the laser pointer and the simulated pointer when performing moves after which the assumption of small angles is not proper and after fast moves that can exceed the sensor full scale range. Nevertheless, when not leaving the operational area, the simulated pointer behaves as the brain would expect it to, thus the application is functional enough to guide the patient to perform a set of predefined moves.

2.1.4 The examination setup

The complete setup is depicted in Fig. 6. The actual laser is still needed for calibration purposes, but is turned off during the examination. Assuming the hospital has a presentation PC with projector it only needs to invest in a device worth about \$50 in components.

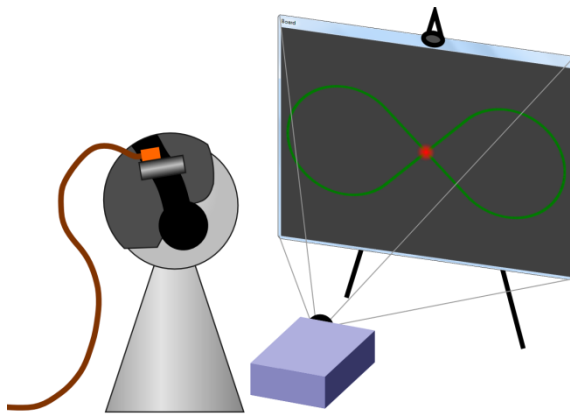


Fig. 6 The proposed examination scheme

2.1.5 System concepts summary

In the designed solution a small device with a gyroscope, accelerometer, magnetometer and laser pointer is fixed to the head of the examined. The sensors gather the information on the elevation, angular velocities of the device and magnetic field lines direction, hence determining the head's position. The shapes and calculated pointer are cast on the screen by means of standard multimedia projector. Before the examination, the system has to be calibrated to account for the change of examined position and location of the screen.

The computer, which coordinates the system, easily obtains the information on the actual spot position in relation to displayed shapes. Since no exhaustive computations are needed, a typical office PC performance is more than sufficient.

2.2. The measurement device

2.2.1 Initial considerations

The sensors box has to be small enough to be mounted on the frame of ear protectors. It should contain the laser pointer on-board and the pointer should be enabled/disabled automatically.

The device should be as light as possible and the cabling should not limit the patient movements in any way. The wireless operation was considered but finally discarded. It would require a costly radio module, define additional requirements of the computer and increase the mass due to the need for battery, which would be the heaviest component. Due to the high popularity and more than sufficient throughput, the USB 2.0 standard was chosen for both data link and power supply.

According to the earlier considerations, the device should have the resolution of 1 mm with the patient located 3 meters away from the screen. Calculation of the appropriate arctangent reveals that the angular resolution should be of about 0.00033 rad (0.02°).

2.2.2 The proof-of-concept hardware

To test if the proposed solution can be implemented successfully, a prototype sensor board, codenamed GyroAccel, was built. The device was fit into the case of a small flashlight. It features a 8-bit accelerometer, 16-bit gyroscope (250 °/s range [5]) and laser pointer.

The device has proven that the idea is useful for the patient examination and encouraged further development. The main disadvantage of the first prototype is too low resolution of the accelerometer.

The schematic of the final revision, v4, is heavily based on the previous prototypes. Minor improvements were made, the board has been redesigned to adopt to the new accelerometer and to fit in a much smaller case, along with the complete laser pointer assembly – see Fig. 7.

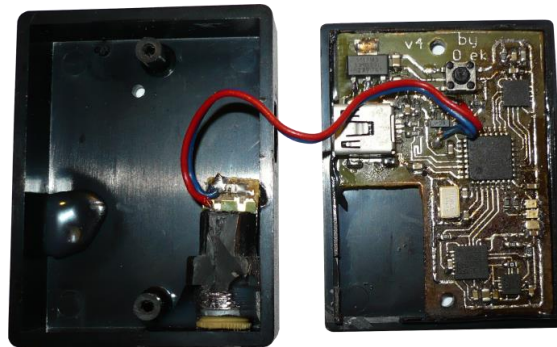


Fig. 7 The final device integrated with laser pointer

All the prototypes were developed around ATMEGA32U2 microcontroller from ATMEL. It is an affordable 8-bit core processor accompanied with 32 KB of FLASH memory, 1 KB of RAM memory and a rich set of peripheral circuits. It has an embedded USB 2.0 Full Speed compatible controller. The microcontroller interfaces accelerometer and magnetometer with an I2C compatible two wire interface and the gyroscope using four-wire SPI bus.

2.3. The data processing

2.3.1 System outline

The hardware part of the system captures the data from the physical sensors and realizes the oversampling required for obtaining a valuable accelerometer readout. Packets, containing the values read from gyroscope, accelerometer and magnetometer are transferred through the USB pipe. The computer receives the data stream of the inertial sensors and passes through the calibration module. The magnetometer's data stream is also extracted, but in the current software revision is not used.

The accelerometer data are used for calculating absolute elevation angle using arcsine. The output from gyroscope is integrated to obtain values of rotation in vertical and horizontal plane. If no calibration would be done previously, the DC component of integrated signal would lead to a drift of the calculated angles.

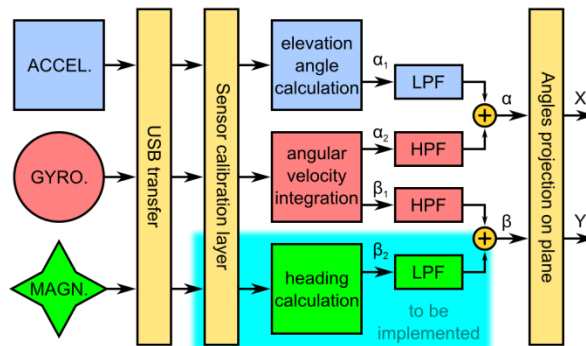


Fig. 8 Data processing scheme

2.3.2 Microcontroller software design

The economic one-sided PCB design process has put several constraints on the microcontroller I/O usage. The SPI lines had to be routed through some other pins to be able to reach the dedicated lines of built-in SPI block. Furthermore, the microcontroller does not offer a hardware

support for the I2C protocol, hence the software solution was adopted.

The application sets the accelerometer for the 800 Hz operation. It collects all the readouts and averages them appropriately to obtain the 14-bit result out of 12-bit samples. The gyroscope and magnetometer readouts are also acquired and a complete matrix of nine 16-bit values is stored in the local FIFO. When the USB controller receives a read request from the host, the data are passed to the USB endpoint buffer and marked for transmission. The communication is done using bulk transfers [6].

The device firmware may be upgraded easily, as the microcontroller is equipped with an USB boot loader. The upgrade feature is activated after pressing the dedicated pushbutton, which is hidden inside the plastic case to avoid accidental activation.

2.3.3 The computer application

The computer application is written in the C# language with bindings to libusb library. The project was developed under Windows with the .NET Framework, but should also compile under the Mono framework for Unix-like platforms.

The data arriving from the USB interface are first checked for the valid packet structure. If the check fails, the algorithm skips following bytes until a valid packet is found. The data are then extracted and the sensors saturation detection is performed. Next the data are processed according to Fig. 8. Finally, the application presents the patient

with the screen resembling the one used in the traditional form of examination – depicted in Fig. 9. The trajectory of the move is recorded and every point outside the predefined shape is highlighted.

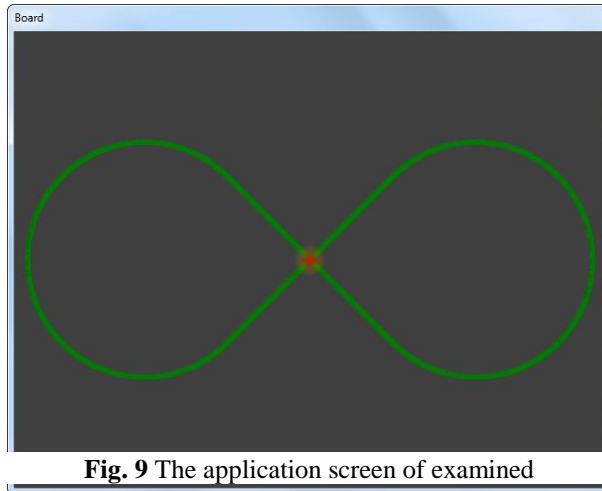


Fig. 9 The application screen of examined

The length of the path outside the shape should be measured together with the maximum deviation to the path. Also the time required to pass between several markers is important and shall be recorded.

The doctor is presented with a simple window for controlling the calibration process and defining visibility of shapes and points of error occurrences.

2.4. The results

The most important objective has been achieved – the developed prototypes proved that the idea of using gyroscope and accelerometer for simulating position of the laser pointer is applicable and can be exploited for building useful medical devices. The cost of parts required for building one prototype is about \$50. The worst-case price of a commercial device could be about \$100, which would still render it an affordable solution for the health care services.

The prototyping process brought forward numerous issues that an engineer has to face constructing similar equipment. The most important is that there are currently no affordable MEMS accelerometers of the resolution higher than 12 bits. Secondly, the simple matrix multiplication based projection may be used only if the strict simulation of the laser pointer is not required and only over a relatively small range of angle values. Nevertheless, its performance may be satisfactory in some cases, mainly if the feedback is provided using simulated pointer instead of the real one.

3. SUDDEN CARDIAC DEATH RISK STRATIFICATION

3.1 Introduction

Sudden Cardiac Death – SCD is a natural death from causes attributable to the heart, preceded by a sudden loss of consciousness within one hour of the onset of acute symptoms in patients with heart disease. Sudden Cardiac Death (SCD) is currently a considerable social issue. According to numerous sources, 30 out of 1 million of population die from SCD every week. In Poland, 1200 SCD related deaths are being classified every week. This

group accounts for 50% of all deaths caused by cardiovascular diseases (Fig. 10). Literature shows that 10 to 32 percent of all natural deaths are sudden deaths and nearly 90 percent of all sudden deaths are classified as SCDs.

Medical conditions that increase the risk of Sudden Cardiac Death occur in broad population of patients. Identification of highest risk cases requires performing a number of clinical tests, such as: coronary perfusion assessment (exercise test, ST segment alteration, angiography), heart failure assessment (NYHA class, ejection fraction, exercise time), autonomic nervous system assessment (heart rate variability, baroreceptors sensitivity) and cardiac dysrhythmia assessment (ambulatory ECG recording, mean ECG, QT segment analysis, exercise test, electrophysiological test). As a result of a limited possibility of high-risk patients' identification, high SCD prevention efficiency of implantable cardioverter defibrillator does not influence directly the overall number of SCDs.

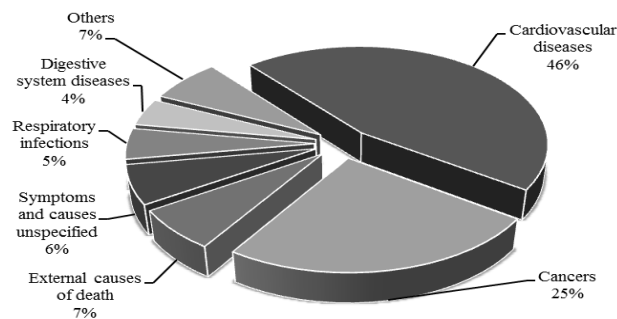


Fig. 10 The share of main causes of the total number of deaths in Poland, 2006

Recently, several markers on the basis of the ECG signal were developed that pose a high prediction value for SCD. Among these markers are T-wave alternans (TWA) [7, 8], heart rate variability (HRV) [9], heart rate turbulence (HRT) and deceleration capacity (DC) [10, 11, 12].

A number of other parameter analyses are implemented in the described project. Every single analysis is designed as an independent plug-in. The use of additional software package for ECG analysis of all patients imposes only a minimal cost in clinical practice, and it can be employed along with the currently used diagnostic software. Additionally, the modular structure of the software and its source code availability simplify the task of potential development and introduction of new algorithms for ECG analysis.

3.2 The functional structure of the platform

Software platform is implemented using Java technology. This fact allows to the use of platform in any popular operating system. It is designed in a modular manner (Fig. 11). The addition of various functionalities can be done by a plug-in software – without the necessity of rebuilding and modifying the main source code. As a result, the platform is a very convenient tool for performing complex research and test of different algorithms for ECG analysis.

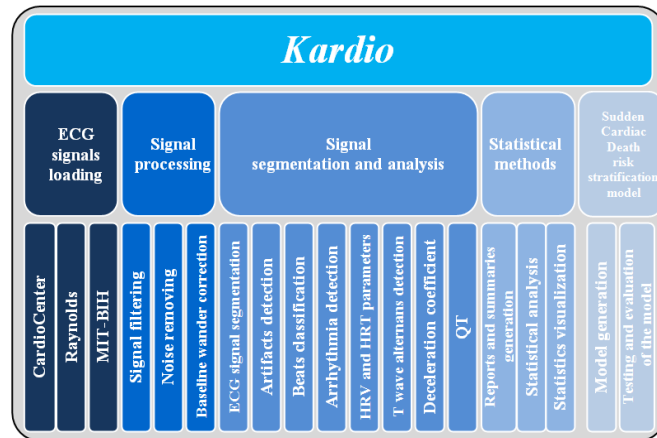


Fig. 11 A block diagram of *Kardio* application.

Platform functionality is divided into following modules.

Patient database

- registration of results from numerous medical examinations and tests (i.e. blood pressure, complete blood count, etc.);
- patients registration;
- visualization of patients condition history;
- patients and results search according to various criteria age, sex, time of day, etc.

Signal acquisition

- importing Holter recordings from various file formats.

Initial preprocessing

- ECG signal filtering using FIR and IIR filters (including zero-phase approach);
- Baseline wandering extraction with both spectral and time-domain (curve subtraction) methods.

ECG signal segmentation and analysis

- heartbeat separation and segment identification;
- artefact and arrhythmia detection;
- heartbeat classification based on previously prepared templates ;
- HRT, HRV, DC (AC) and TWA (with MMA and spectral methods) assessment.

Statistical module

- reports generation for a given group of patients;
- statistical analysis of marker dynamics in accordance to various criteria.

Model generation module

- model extraction based on optimization of: sensitivity, positive predictive accuracy, negative predictive accuracy and specificity [13, 14].

3.3 Risk stratification models

An essential element of the application is the possibility of risk stratification model generation. The models are implemented as plug-ins so the authors have many possibilities of the application development. The authors performed research based on various artificial intelligence models. Finally, four classification support models were selected and implemented in the presented platform.

Simple model – logical conjunction

The simplest concept implemented by authors is based on using one or more parameters. Conditions for the various parameters are combined using a logical conjunction [15]. Geometrically, this is consistent with a cut in a single area of the search space which is characterized by an increased risk of disease.

Decision tree

The second approach is based on decision trees. Decision tree is a graph in which the vertices correspond to the tests – a comparison of the values of attributes, arcs to the test scores, and leaves to the classes. The apex of the tree is called the root of the tree. Each internal vertex of a decision tree consists of the division, which is responsible for the division of the data set to the appropriate partition. A partition can be understood as a set of data belonging to one class, resulting from the division of the training set.

Bayesian network

The third approach is based on Bayesian network which is an advanced form of a probabilistic approach based on Bayesian reasoning [14]. This approach is widely used in many medical applications. Bayesian network consists of a directed graph describing the qualitative relationship between events and their numerical specification.

Artificial neural network

The Artificial Neural Network is the most known technique for making diagnosis based on using an expert system (which is a branch of artificial intelligence). Artificial Neural Networks were inspired by biological findings relating to the behaviour of the brain as a network of units called neurons. In this research authors use artificial neural networks to classify heart diseases. In order to do that multilayer feed forward neural network has been chosen.

3.4. Summary

Project results:

- Sudden Cardiac Death risk stratification based on Holter ECG monitoring;
- Software platform (open and generally available) for ECG signal analysis and patients management with statistical reporting facilities. Software has a plug-in architecture. Thanks to this it is easy to extend its features and make further improvement. Software (together with the source code) is royalty free. This can contribute to acceleration of the research on ECG analysis;

- ECG signal processing algorithms, especially segmentation and segments identification adjusted for data from vital function monitors and Holter recorders;
- The authors have prepared an advanced platform based on plug-ins architecture. The developed application enables a user to generate simple and advanced risk stratification models including: neural networks, Bayesian networks, decision trees.

4. THERMOGRAPHIC ASSESSMENT OF BURN WOUND DEPTH IN CHILDREN

4.1. Introduction

One of the most important clinical problems of children burn treatment is the early and accurate evaluation of the burn wound depth and the determination of the necrosis limits. This evaluation influences the decision of a surgeon whether to operate a patient. The less serious wounds can heal in a natural way, but the more severe ones, have no chance of tissue regeneration, because of the necrosis [16,17]. This kind of wounds requires excision of necrotic tissues with the concurrent split thickness skin graft. The ideal solution would be to provide surgeons with adequate tools allowing early classification of the burn wound depth and providing them with a kind of wound map indicating clearly the areas to be operated on.

Obviously, there exist diagnostic methods such as clinical assessment by a physician or the evaluation of the biopsy material, but the first one is subject to human errors and is very difficult during the first days after a thermal injury, while the second one is invasive and painful for patients. The use of infrared thermography in medicine is not an entirely new idea [18,19], but the recent advances in the infrared technology and the image processing techniques allow significant improvements in diagnostics.

4.2. Physiological foundations

The current practice in the assessment of the burn wound depth is based on the evaluation of a wound by a surgeon and the results of a biopsy, which is an invasive examination. Thus, the goal of the current research would be to reduce the influence of the human factor on the results of the wound classification and to limit the number of required biopsies.

The use of infrared thermography is possible because the microcirculation of blood in the burn wound tissues is changed, which is reflected in the skin temperature. Consequently, the analysis of skin temperature differences within the registered infrared images should render possible the classification of burn wound depth by segmenting each image into individual areas having the same range of temperatures. The segmentation process could be based on the analysis of temperature histograms of the registered infrared images, which is a well-known approach already discussed in the literature [20,21].

An important element is to establish the standard procedure to perform infrared measurements. In the proposed method the infrared images of a wound are taken 24 and 72 hours after the thermal injury. Later the evaluation of the burn depth would not be possible because of the inflammatory processes which change the original temperature distribution within the wound resulting from the blood vessels damage. Before each measurement, the patient is anesthetized and undressed for several minutes to let the thermoregulation processes equalize the skin temperature (see Fig. 12).

The evaluation of a wound is validated each time with a number of traditional biopsies, which are taken in the locations indicated by a surgeon. After the thermographic method is proved correct, the number of biopsies may be reduced, or they may be dispensed with altogether.

4.3. Image capture system

The image capture system, whose general view is shown in Fig. 12, is based on the modern bolometric infrared camera FLIR P660. The camera features the built-in visible light channel allowing an operator the automatic overlay of the visible image with the infrared one. Both images can be recorded in a single JPEG file on the built-in card or transmitted in real time to a PC through a fire-wire interface.

The storage and the transmission of data in the system complies with the regulations concerning medical images, in particular with the Digital Imaging and COmmunication in Medicine (DICOM) standard, which regulates the handling, storing and transmission of information in medical imaging. The DICOM standard, known as the ISO 12052:2006 standard, is commonly used in hospitals. It includes a file format definition and a TCP/IP based network communications protocol.

Owing to the adoption of the DICOM standard, files containing all the patient data and medical images can be exchanged between various health-care institutions. The DICOM standard also enables integration of hardware provided by various manufacturers, such as scanners, servers, workstations, printers, into a single medical database, known as the Picture Archiving and Communication System (PACS).



Fig. 12 Recording of the burn wound thermographic image using FLIR P660 camera

4.4. Dedicated software

Although the employed infrared camera is accompanied by PC software for image processing, the functionality of this software is not adequate for the task of wound classification. Consequently, one of the main tasks in the presented project was to develop a custom PC software solution, performing comprehensive analyses needed to correctly classify the wound. The aim was to develop a solution that would be easy to use, yet provide the complete processing path – from the captured images serving as the input data, to the detailed report containing indications for further treatment forming the output.

The developed software, named BurnDiag, is intended to work with two types of images: thermovision and visible light. The main input is the thermovision image, the visible light one is supplemental, providing means to map burn wound areas to the body areas as seen by the human eye. Both images are read from a disk (usually a memory card of the camera). Although it would be possible to use a direct connection with the camera, this would require additional cables, which are an unwelcome addition during patient examination.

The user interface is able to display both images side-by-side, making their comparison straightforward. Apart from the images, the program main window contains controls (buttons, edit boxes, etc.) required for performing analyses and displaying their results (Fig. 13). The interface can also be switched to text view, displaying textual information about the patient and the wound. These data are stored in a database. The images may be stored in DICOM format [22].

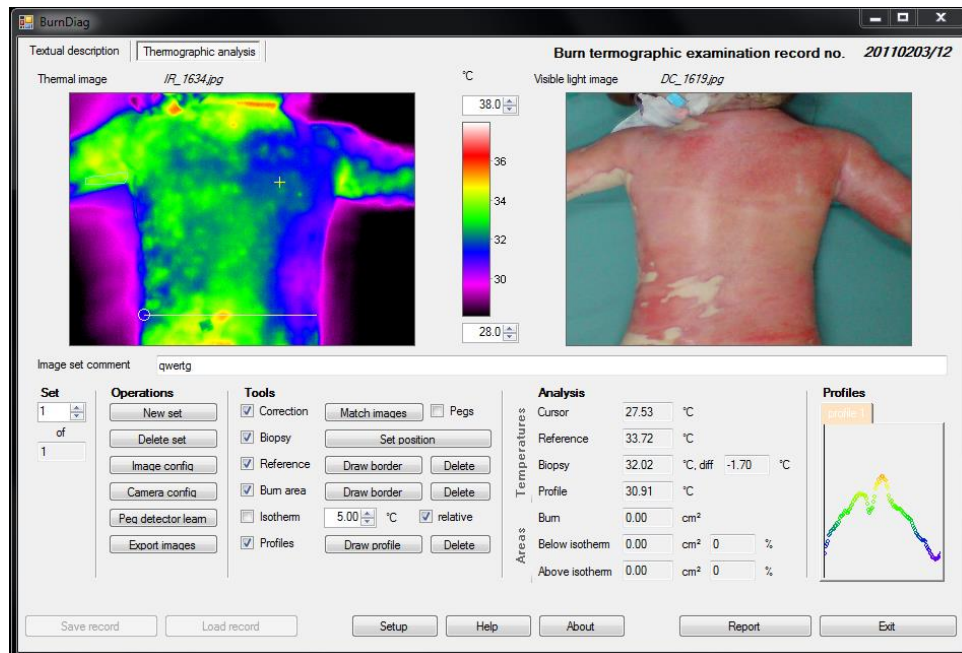


Fig. 13 Interface of the BurnDiag software (image analysis tab)

The software is able to read thermographic images in FLIR jpg format and also visible light images in standard jpg format. The FLIR jpg image format is a proprietary format that can be read by general-purpose graphical imaging software – in this case only the false color snapshot is available. However, it can also be processed by a dedicated library made available by FLIR – in such case the file exposes temperature data for the whole area of the image (as an array of C language float data type objects) and also some useful information about the conditions present when the image was taken. The presented software uses the second approach.

The software supports following operations on the thermographic image:

- presenting image in user-selected false colour palette,
- adjusting lower and upper temperature limit,
- freehand drawing of a closed path in order to delimit the wound area or the temperature reference area,
- setting the point of (optional) biopsy and reading its temperature,
- displaying an isotherm and computing burn area having temperature below and above the isotherm,
- displaying temperature profiles along user-drawn lines.

It also allows matching the visible light image to the thermographic one, generate final reports in Adobe PDF or Microsoft Word doc format and export images in popular formats.

Matching the visible and thermographic images, mentioned in the preceding paragraph, is essential for obtaining meaningful results of analyses: the analyses are performed on the thermographic image, but the indications for surgery have to be presented in the visible light image. In order to transfer results from the thermographic image to the visible light one, both images should be taken from the same point in space and using cameras with exactly the same angle of view.

In practice, these conditions are never met. Even when thermovision – visible light combo camera is used (such as the FLIR ThermaCam P660), the lenses of the two cameras are separate and offset by several centimetres, they angles of view are also vastly different (the angle of view of the visible light camera being usually much wider). This problem is illustrated in Fig. 14, which presents the thermographic and visible light images of the same object. When separate thermovision and visible light cameras are used, the problem becomes even more obtrusive, due to possible rotation of the cameras.

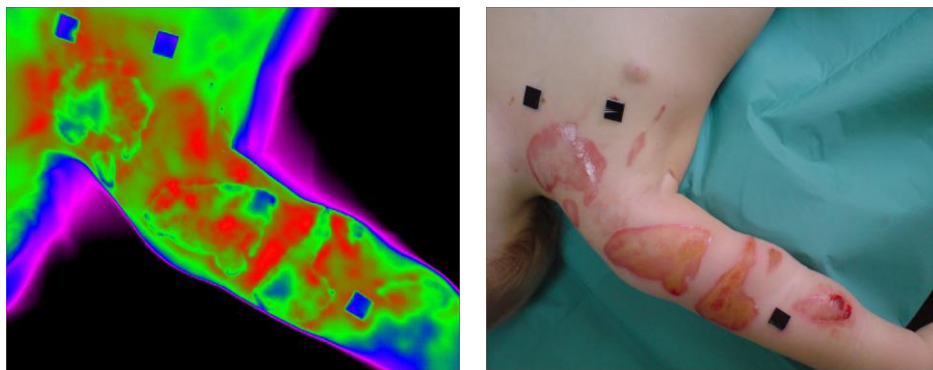


Fig. 14 Thermographic and visible light image of the same object.

Note the different position of the uppermost reference markers (black squares)

In order to match (register) the image with the other one, two distinct steps are required: a) determining corresponding points in the images, b) applying suitable transformations. If a number of point pairs in the images being matched can be identified that correspond to the same objects in the recorded scene, then it is possible to compute image transformation coefficients. The more pairs are identified, the more parameters can be used in the transformation process, and therefore more complicated deformations can be corrected. BurnDiag employs three pairs of points, which allow performing affine transform.

The points in question could be selected in various ways, ranging from manual identification to fully automatic approach that includes discovery of the features of the images that can be treated as reference points. For the purpose of BurnDiag software, a solution has been proposed that performs automatic detection of reference points in the images, but the points themselves are marked by placing predefined shapes on the investigated object (human body in this case). This offers more robust performance and less chance of errors, which in case of medical diagnosis are particularly unwanted. The mentioned predefined objects are black squares with area of 1 cm^2 each. Moreover, the reference objects are used in computations of the wound area: because their area is exactly 1 cm^2 , they allow the software to calibrate the algorithm for area computation.

The detection procedure consists of several steps and is similar for both the thermographic and visible light image. However, the former requires additional considerations, which will be covered towards the end of this subsection.

The first step of the procedure is conversion of the image to a grayscale equivalent. Next, an edge detection procedure is applied, allowing for disclosing objects which differ significantly in brightness from the surroundings – in this case the reference squares. This is followed by a sequence of dilatation and erosion filters – the purpose is to expose distinct objects in the image and increase the chance they will be outlined by a closed path. The dilatation filter grows the objects in the image, consequently filling the gaps that may appear in the path outlining the reference squares. The erosion filter removes small stand-alone objects, which reduces noise and smoothes the outline of the squares. Then, the resulting pre-processed images are passed to the blob detector which labels regions corresponding to individual objects larger than a predefined threshold area. This algorithm produces a list of large objects including the three black squares. The next step is the exclusion from the list of the objects which significantly differ from the square shape. For this purpose, every object in the list is tested for being quadrilateral and having sides and angles of similar values. The objects which pass the test are sorted by their area. The final step of the algorithm is the search through the list of remaining objects for three shapes having similar areas. When such a set is found, the entire detection procedure is finished.

Before the actual image transform can be performed, the reference points in infrared images have to be related to their counterparts in visible light images. For three reference points in a figure, there exist six possible ways of pairing the identified points. Thus, in order to select the correct solution, the Euclidean distances between the points of interest are calculated in both types of images. Then, for each pairing, the sum of distances between the points is computed and the solution producing the lowest sum of distances is selected as the correct one. This approach is justified when the mutual rotation between images is not significant, which is true in the considered case.

Finally, the three pairs of points matched in the above-described procedure allow the execution of an affine transform, i.e., a transform that can map a parallelogram onto

square [23]. Numerous tests carried out on real images registered for burn wounds located in different parts of a human showed that this kind of transform is sufficient for the considered application. As far as the choice of a particular image to be transformed is concerned, it should be underlined that it is the visible light image which should undergo the transformation because, for medical diagnosis reasons, the infrared one should not be subject to any unnecessary processing. The result of the fully automatic correction procedure, presenting the transformed image from Fig. 14, is shown in Fig. 15.

It should be noted that processing thermographic images by the described algorithm may be troublesome due to their very low spatial resolution (compared to the typical visible light image). At 640×480 pixels the reference squares may be too small for reliable detection. It has also been observed that the depth of field for the thermographic camera was small, which led to the squares (placed outside of the wound, and as a result, often at different distance from the camera than the fragment on which the camera focused) being out of focus. To handle such situations, the BurnDiag software allows also manual (by mouse click) marking of the reference squares in the images.

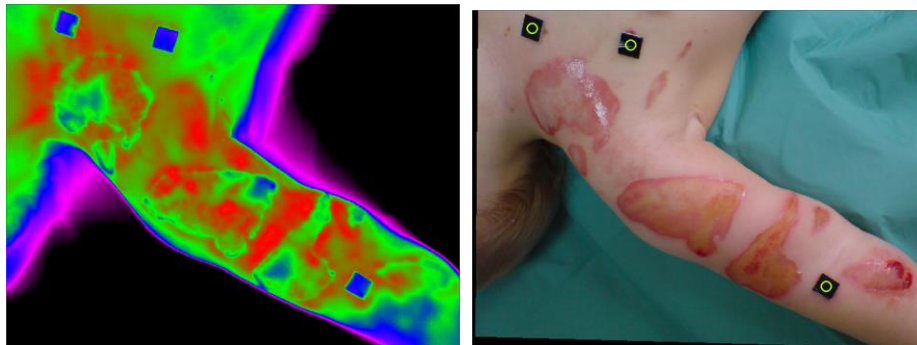


Fig. 15 Thermographic and visible light image of the same object.
The visible light image is corrected to match the thermographic one

4.5. Medical results

Each time the infrared assessment of a burn wound was validated with a number of standard biopsies, which were taken only in the locations indicated by a surgeon and marked in infrared images by sterile pads of a diameter comparable with the one of the needle used for the biopsy. The infrared assessment of the burn wound depth showed extremely high correlation with the histopathological evaluation of the biopsy material and the clinical assessment of a wound by a physician. The results demonstrate that the temperature of superficially burned wound is only slightly changed with respect to the undamaged skin surrounding the wound. On the contrary, the deeply burned skin has the temperature lower by more than 3 K. As far as the optimal temperature thresholding value used for the separation between the burns of degrees IIa and IIb is concerned, the experimental results show that this value should be located approximately 1.45 K below the healthy skin temperature. This important result has been proven on a statistically sound number of clinical cases.

When setting the precise temperature thresholding value, one should keep in mind that if this value is set too low, some of the necrotic tissues will not be removed during a surgery and the grafting will have to be repeated. Hence, it is much safer to set this value at a bit higher level than required. Then, patients will not have to undergo an additional surgery.

4.6. Conclusions

This chapter presented a new possible clinical method for the classification of the burn wound depth based on the analysis of infrared images. This method seems to be promising and compared to the traditional biopsy it is contactless and non-invasive, thus it is much more tolerable for young patients and brings very much same results from the diagnostic point of view. Additionally, the proposed method largely eliminates the human factor from the diagnostic process and the results do not depend on a particular person performing the diagnostics or his/her current condition.

The presented research combined the quantitative thermographic examination of burn wounds in children with the original quantitative histometrical assessment of biopsy punches taken at the same time from the examined wounds, hence proving to our best knowledge for the first time the high correlation between these two investigation methods; non-invasive thermography and invasive histopathology.

Consequently, it has been made possible to draw the exact isotherm dividing a burn wound area into two parts: superficially and deeply damaged, hence offering to surgeons a new non-invasive instrument to create maps of burn wounds which allows them to make the correct, early and exact decision: to operate or not to operate on the patient. Moreover, such thermographic maps of burn wounds resulting from examinations are exact plans for surgical operations indicating places within the wound where necrotic tissues must be excised and places where surgical intervention is not required. It is also worth mentioning that the developed software for the analysis of burn wounds in children allows the complete and objective documentation of thermal injuries; including the storage of infrared and visible light images, the course of medical treatment and, most importantly, it supports making the therapeutic decision which is the best for the patient.

Concluding, the main benefits of the present clinical research are as follows:

- it allowed the determination of the correlation between the change of skin temperature and the degree of burn depth (especially IIa and IIb) by comparing the results of biopsy evaluation with the infrared images in a statistically sound number of cases hence allowing significant reduction, if not complete elimination, of the number of biopsies required and consequently relieving the patient and speeding up the process of burn depth evaluation;
- it facilitated fully automatic correlation and fusion of infrared and visible light images which are taken by the same or different camera with different fields of view and depth of focus. The developed software allows not only off-line analyses and reporting of recorded images, but it is a real time tool used to process and analyze the images which produces the wound maps used during grafting and calculating the surface of the wound.

Further research in this area will be focused on the precise determination of the temperature value which should be used for the thresholding of the infrared images. Tests in hospital environment will determine the need for subsequent improvements of the developed software.

Acknowledgements: *The researches presented in the paper were supported by:*

- *funds from the National Science Centre granted on the basis of the decision number No. UMO-2011/03/B/ST6/03454,*
- *funds from the Polish Ministry of Scientific Research and Higher Education granted on the basis of the decision number No. N5 15 2423 37*

Authors would like to thank the following researchers: Professor Małgorzata Kurpesa MD, PhD, DSc, Ewa Trzos MD, PhD, DSc, Urszula Cieślak-Guerra MD, Barbara Uznańska-Loch MD, and Wojciech Kuzanski MD, PhD.

REFERENCES

- [1] Z. Ciota: "Design and Realization of Smart Speech Processors". In Proceedings of the 15th IEEE International Conference on Electronics, Circuits, and Systems, ICECS 2008, Malta, 31st August - 3rd September 2008.
- [2] D. Krzesimowski, Z. Ciota: "Signal Processing of Voice in Case of Patients After Stroke", *Przegląd Elektrotechniczny (Electrical Review)*, no. 11, 2010, pp.129-132
- [3] D. Krzesimowski, Z. Ciota: "Estimation of Hospitalization Progress for Patients with Stroke with Using of Voice Analysis" In Proceedings of the 6th Int. Workshop on Models and Analysis of Vocal Emissions for Biomedical Applications, Firenze, Italy, December 14-16, 2009
- [4] Winter David: *Biomechanics and motor control of human movement*, chapter 7, University of Waterloo, 1999 Waterloo, Ontario, Canada
- [5] STMicroelectronics: L3G4200D ultra-stable three-axis digital output gyroscope
- [6] Compaq, Hewlett-Packard, Intel, Lucent, Microsoft, NEC, Philips: *Universal Serial Bus Specification*, Revision 2.0, April 27, 2000
- [7] Kamiński M., Chłapiński J., Sakowicz B., Kotas R.: „ECG Signal Processing for T-wave Alternans Detection”, pp. 623-628, 16th International Conference Mixed Design of Integrated Circuits and Systems MIXDES 2009, 25-27 June 2009, Lodz, Poland, wyd. Tech. Univ. Łódź, DMCS, Poland, form. A4. s.722, ISBN 978-83-928756-0-4
- [8] Chłapiński J., Kamiński M., Sakowicz B., Kotas R.: "T-wave Alternans Analysis In Ambulatory ECG Monitoring", pp. 229-232, Proceedings of the Xth International Conference TCSET'2010, "Modern Problems of Radio Engineering, Telecommunications and Computer Science", Lviv-Slavsko, Ukraina, 23-27 February 2010, s.380, A4, wyd. Publishing House of Lviv Polytechnic National University 2010, ISBN 978-966-553-875-2
- [9] Cieślak-Guerra U., Kamiński M., Kotas R., Rechciński T., Wadolowska E., Jerka K., Uznańska-Loch B., Trzos E., Kasprzak J.D., Kurpesa M.: „Effect of cardiac rehabilitation on time and frequency domain analysis of heart rate variability and coronary syndrome (Forever study)", ESC Congress 2014, 30 Aug 2014 - 03 Sep 2014 Barcelona
- [10] Kamiński M., Chłapiński J., Sakowicz B., Kotas R. , Napieralski A.: „ECG Signal Processing for Deceleration Capacity Assessment" *Elektronika – Konstrukcje, Technologie, Zastosowania*, Grudzień 2011, nr 12/2011, ISSN 0033 -2089
- [11] Kamiński M., Chłapiński J., Sakowicz B., Kotas R.: "ECG Signal Processing for Deceleration Capacity Assessment", pp.657-662, 18th International Conference Mixed Design of Integrated Circuits and Systems MIXDES 2011, Gliwice, 16-18 June 2011, wyd. Tech. Univ. Łódź, DMCS, Poland, form. A4. s.702, ISBN 978-83-932075-0-3
- [12] Kamiński M., Chłapiński J., Trzos E., Kurpesa M., Napieralski A.: „Differentiation of the Deceleration Capacity marker for periods of sleep and wakefulness" - XIV Międzynarodowa Konferencja Wspólna International Society for Holter Monitoring and Noninvasive Electrocardiology oraz Sekcji Elektrokardiologii Nieinwazyjnej i Telemedycyny Polskiego Towarzystwa Kardiologicznego, 2012
- [13] Marciniak P., Kotas R., Kamiński M., Ciota Z., „Implementation of artificial intelligence methods on the example of the risk stratification of cardiovascular diseases", 21th International Conference Mixed Design of Integrated Circuits and Systems MIXDES 2014, 19-21 June 2014, Lublin
- [14] Kamiński M., Kotas R., Mazur P., Sakowicz B., Napieralski A.: "Optimization model for risk stratification of sudden cardiac death", 20th International Conference Mixed Design of Integrated Circuits and Systems MIXDES 2013, 20-22 June 2013, Gdynia

- [15] Kamiński M., Kotas R., Mazur P., Sakowicz B., Napieralski A.: „Models for Risk Stratification of Sudden Cardiac Death Based on Logical Conjunction and Decision Tree”, *International Journal of Microelectronics and Computer Science*, 2013, 2080-8755, 2013, nr 2, s. 65-71
- [16] Heimbach D., Emgrav I., Grube B., Marvin J, “Burn depth: a revive”. *World J. Surg.* 16, pp. 10-15, 1992
- [17] Hendricks W. M, “The classification of burns.” *J. Am. Acad. Dermatol.*, n.5, 1990
- [18] Mason B.R., Graff A.J., Pegg S.P., “Colour thermography in the diagnosis of the depth of burn injury.”, *Burns Incl. Therm. Inj.*, 7, 197, 1981
- [19] Cole R.P., Jones S.G., Shakespeare P.G., “Thermographic assessment of hand burns.”, *Burns*, 16, pp. 60-63, 1990
- [20] Glasbey C.A., “An analysis of histogram-based thresholding algorithms.”, *Comput. Vis. Graph. Image Process.*, Vol. 55, pp. 532-537, 1993.
- [21] Pal N.R., Pal S., “A review on image segmentation techniques.”, *Pattern Recognition*, Vol. 26, pp. 1277-1294, 1993.
- [22] DICOM specification, <ftp://medical.nema.org/medical/dicom/2009/>
- [23] Zitova B., Flusser J., "Image registration methods: a survey", *Image and Vision Computing*, vol. 21, No. 11, pp. 977-1000, 2003